

Aberystwyth University

Saprotrophic proteomes of biotypes of the witches' broom pathogen *Moniliophthora perniciosa*

Pierre, Sandra; Griffith, Gareth; Morphew, Russell; Mur, Luis; Scott, Ian

Published in:
Fungal Biology

DOI:
[10.1016/j.funbio.2017.05.004](https://doi.org/10.1016/j.funbio.2017.05.004)

Publication date:
2017

Citation for published version (APA):

Pierre, S., Griffith, G., Morphew, R., Mur, L., & Scott, I. (2017). Saprotrophic proteomes of biotypes of the witches' broom pathogen *Moniliophthora perniciosa*. *Fungal Biology*, 121(9), 743-753.
<https://doi.org/10.1016/j.funbio.2017.05.004>

General rights

Copyright and moral rights for the publications made accessible in the Aberystwyth Research Portal (the Institutional Repository) are retained by the authors and/or other copyright owners and it is a condition of accessing publications that users recognise and abide by the legal requirements associated with these rights.

- Users may download and print one copy of any publication from the Aberystwyth Research Portal for the purpose of private study or research.
- You may not further distribute the material or use it for any profit-making activity or commercial gain
- You may freely distribute the URL identifying the publication in the Aberystwyth Research Portal

Take down policy

If you believe that this document breaches copyright please contact us providing details, and we will remove access to the work immediately and investigate your claim.

tel: +44 1970 62 2400
email: is@aber.ac.uk

Accepted Manuscript

Saprotrophic proteomes of biotypes of the witches' broom pathogen *Moniliophthora perniciosa*

Sandra Pierre, Gareth W. Griffith, Russell M. Morphew, Luis A.J. Mur, Ian M. Scott



PII: S1878-6146(17)30054-5

DOI: [10.1016/j.funbio.2017.05.004](https://doi.org/10.1016/j.funbio.2017.05.004)

Reference: FUNBIO 816

To appear in: *Fungal Biology*

Received Date: 29 September 2016

Revised Date: 3 May 2017

Accepted Date: 16 May 2017

Please cite this article as: Pierre, S., Griffith, G.W., Morphew, R.M., Mur, L.A.J., Scott, I.M., Saprotrophic proteomes of biotypes of the witches' broom pathogen *Moniliophthora perniciosa*, *Fungal Biology* (2017), doi: 10.1016/j.funbio.2017.05.004.

This is a PDF file of an unedited manuscript that has been accepted for publication. As a service to our customers we are providing this early version of the manuscript. The manuscript will undergo copyediting, typesetting, and review of the resulting proof before it is published in its final form. Please note that during the production process errors may be discovered which could affect the content, and all legal disclaimers that apply to the journal pertain.

Saprotrophic proteomes of biotypes of the witches' broom pathogen

Moniliophthora perniciosa

Sandra PIERRE[†], Gareth W. GRIFFITH, Russell M. MORPHEW,
Luis A.J. MUR, Ian M. SCOTT*

Institute of Biological, Environmental and Rural Sciences, Aberystwyth University,
Ceredigion, SY23 3FG, UK

*Corresponding author. Institute of Biological, Environmental and Rural Sciences,
Aberystwyth University, Ceredigion, SY23 3FG, UK. Tel.: +44 (0)1970 622325; fax: +44
(0)1970 622350

[†]Deceased

E-mail address: gwg@aber.ac.uk

ABSTRACT

Nine geographically diverse isolates of the witches' broom pathogen *Moniliophthora perniciosa* were cultured on nutrient medium. They included six C-biotype strains (from five tropical American countries) differing in virulence on the cacao plant *Theobroma cacao*, two Brazilian S-biotypes, infective on solanaceous hosts, and an Ecuadorian L-biotype, infective on certain lianas. Mycelial growth rates and morphologies differed considerably between the strains, but no characters were observed to correlate with virulence or biotype. In plant inoculations using spores from basidiome-producing cultures, one C-biotype caused symptoms on tomato (an S-biotype host), thereby adding to evidence of limited host adaptation in these biotypes. Mycelial proteomes of the nine strains were analyzed by two-dimensional gel electrophoresis (2-DE), and 619 gel spots were indexed on all replicate gels of at least one strain. Multivariate analysis of these gel spots discriminated the L-biotype, but not the S-biotypes, from the remaining strains. The proteomic similarity of the S- and C-biotypes could be seen as consistent with their reported lack of phylogenetic distinction. Sequences from tandem mass spectrometry of tryptic peptides from major 2-DE spots were matched with *Moniliophthora* genome and transcript sequences on the NCBI and Witches' Broom Disease Transcriptome Atlas databases. The protein-spot identifications indicated the *M. perniciosa* saprotrophic mycelial proteome expressed functions potentially connected with a 'virulence life-style'. These included peroxiredoxin, heat-shock proteins, nitrilase, formate dehydrogenase, a prominent complement of aldo-keto reductases, mannitol-1-phosphate dehydrogenase, and central metabolism enzymes with proposed pathogenesis functions.

*Key words:**Moniliophthora*

Mycelia

Proteome

Tandem mass spectrometry

Two-dimensional electrophoresis

Witches' broom disease

Introduction

The causal agents of the two major diseases of cacao (the source of cocoa for chocolate) in tropical America are sister taxa in the agaric genus *Moniliophthora* (Griffith *et al.* 2003; Aime and Phillips-Mora 2005). Due to their economic impact and global threat, much research has been devoted to the genomes of both species, *M. perniciosa* (Mondego *et al.* 2008) and, more recently, *M. roreri* (Meinhardt *et al.* 2014; Díaz-Valderrama and Aime 2016). Genome information has underpinned recent studies on transcripts expressed *in vitro* or *in planta* during the *M. perniciosa* life-cycle, by revealing or confirming potential pathogenesis and developmental functions (Pires *et al.* 2009; Leal *et al.* 2010; De Oliveira *et al.* 2012; Thomazella *et al.* 2012; Franco *et al.* 2015; Gomes *et al.* 2016).

Transcript expression does not necessarily equate to protein content, and therefore the technically more challenging proteomics approach has also been applied to many plant pathogenic fungi (Fernández-Acero *et al.* 2006, 2007; Böhmer *et al.* 2007; Cobos *et al.* 2010; Kwon *et al.* 2014). *Moniliophthora* proteomics should be another beneficiary of relevant genome resources. Silva *et al.* (2012) have described an early proteomic study of *M. perniciosa*.

The present study applied proteomics to *in vitro* cultures of *M. perniciosa* (formerly *Crinipellis perniciosa*). As a hemibiotroph, *M. perniciosa* grows saprotrophically on standard nutrient media. One of our objectives was to gauge whether the proteome of this culturable form contained only ‘housekeeping’ proteins, or whether its latent pathogenicity was evident in specialist functions that could be recognized with the aid of genome information.

A related query was whether genotypic diversity of *M. perniciosa* isolates, differing in host range and virulence, might manifest in the saprotrophic proteome. *M. perniciosa* is indigenous to the Amazon region but, over this vast territory, geographically separated populations infecting a range of host plants have been identified (Meinhardt *et al.* 2008). The important ‘C-biotype’ infects certain species of the Malvaceae in the genera *Theobroma* (notably the cacao plant, *T. cacao*) and *Herrania*. Symptoms of the biotrophic phase of infection include stem swellings, and the shoot proliferation that engendered the name of witches’ broom disease (Meinhardt *et al.* 2008).

Included in this study were C-biotype isolates differing in their specific virulence interactions with cacao. Shaw and Vandenbon (2007) found the cacao clone Scavina 6,

selected historically for witches' broom resistance, was never infected by the Trinidadian isolate GC-A5. In contrast, two Brazilian isolates, Cast1 and APC3, were both able to infect Scavina 6. All three of these isolates were investigated here, along with other C-biotypes from Ecuador, Peru and Bolivia.

The 'S-biotype' was found by Bastos and Evans (1985) on species of the Solanaceae near cocoa farms in the Amazon. Although S-biotype basidiospores cause witches' broom symptoms in *Solanum lycopersicum* (tomato) and *Capsicum annuum* (bell pepper), *M. perniciosus* has not become an agricultural disease of solanaceous crops (Marelli *et al.* 2009). Interestingly, DNA studies have found the C- and S-biotypes are not phylogenetically distinct (de Arruda *et al.* 2005; Marelli *et al.* 2009).

A third biotype investigated was the 'L-biotype', found in tropical forest on liana vines such as *Arrabidaea verrucosa* of the Bignoniaceae (Griffith and Hedger 1994ab). The outcrossing reproductive strategy (bifactorial heterothallism) of the L-biotype results in greater local genetic diversity than in the C- and S-biotypes, which exhibit primary homothallism (Griffith and Hedger, 1994ab). Most genetic diversity in the latter biotypes appears to be associated with different geographical origins (Ploetz *et al.* 2005; Rincones *et al.* 2006).

Accordingly, this study compared the growth and proteomic profiles in culture of C-biotypes of different geographical origins and reported virulence, S-biotypes and an L-biotype of the witches' broom pathogen *M. perniciosus*. In the process, the utility of recently-available sequence information on the *Moniliophthora* genomes (Mondego *et al.* 2008; Meinhardt *et al.* 2014) and *M. perniciosus* transcriptomes (Teixeira *et al.* 2014) was demonstrated.

Materials and methods

Fungal cultures

Moniliophthora perniciosa strains belonged to our isolates collection (Table 1), stored long-term in 15% glycerol at -80°C. Mycelial cultures were grown at 25°C in the dark, on MYEA medium (5 g yeast extract, 30 g dark malt powder, 15 g agar, per L). Growth was measured from colony radii at two-day intervals between 9 and 13 days after subculture. Agar-free mycelia, when required, were grown in 'top-layer' cultures (Cohen 1973), in which four square plugs (5 × 5 mm) of mycelia from MYEA were inoculated (facing up) on the surface of double-strength MYEA in 9 cm Petri dishes, followed by the addition of 6 mL sterile dH₂O which formed a liquid layer ca. 1 mm deep on the agar surface. Plates were incubated at 25°C in the dark. This method allowed growth of fungal cultures with the same morphology as on standard agar, but with easy removal of the mycelium with a spatula.

Mycelia for protein extraction were harvested from 12 day-old top-layer cultures, washed in water, blotted on filter paper, and samples (200 mg) weighed, then freeze-dried.

Basidiomes were produced by a modified Griffith and Hedger (1993) method. A bran-vermiculite mixture (40 g vermiculite, 50 g domestic bran cereal, 6 g CaSO₄(H₂O)₂, 1.5 g CaCO₃, 200 mL distilled water) was distributed into six domestic aluminium pie dishes (110 mm diameter × 20 mm deep), sealed with aluminium foil and autoclaved (15 min, 120°C). Each pie dish was inoculated in sterile conditions with eight mycelial pieces (0.5 × 1 cm) from 2-3 week-old top-layer cultures (placed with aerial mycelia face-down), then re-sealed with foil and incubated at 25°C in a vented plastic container, until the bran-vermiculite matrix was covered by dense white mycelium (typically three weeks). The pie-dish cultures were then hung with wire (Vaseline-coated to exclude pests) on a rail in a vented Plexiglass mist cabinet (50 cm × 50 cm cross-section, 1 m height, held on 30 cm legs above a timer-controlled humidifier), in a warm glasshouse (18-28°C). Pie-dish cultures were kept in constant mist until basidiome primordia appeared (about 10 days), then transferred to periodic misting, typically two daily periods (01:00-08:00 h and 16:00-17:00 h).

Plant inoculations

To harvest basidiospores, pilei from fresh basidiomes (8-25 mm diameter) were pinned to a polystyrene support, gills facing down, over a film of slurry agar (1 mL of 0.2% agar no. 2,

autoclaved) in a 9 cm Petri dish. Sufficient pilei were mounted for complete coverage of the Petri dish, and left for 3-6 h. The agar bearing visible spore prints was scraped into a 2 mL centrifuge tube, gently homogenized, and adjusted to 10^6 spores mL^{-1} .

Plants were grown in pots of peat-based compost. Cacao (*Theobroma cacao* cv. Comum) was inoculated at two months old. Tomato (*Solanum lycopersicum* cv. Ailsa Craig) plants were inoculated at 10-14 days old. Spore suspensions (20-40 μL) were placed onto apical buds and the top three axillary buds. A second inoculation was applied after 3 days. Controls were mock-inoculated with spore-free agar. Inoculated plants remained 2-3 days in a warm (30-45°C), humid micro-climate in trays of 1 cm-deep water covered with clear plastic hoods and placed over heating pipes. The hoods were then removed, and the plants kept in a warm (20-45°C) glasshouse with saturating relative humidity.

Protein extraction

Each strain was extracted in biological triplicates (i.e., three culture experiments). Freeze-dried mycelial samples were ground with mortar and pestle, cooled on ice with 2 mL extraction buffer, containing 16 mM K_2HPO_4 , 4 mM KH_2PO_4 , 1% Triton, 33 mM dithiothreitol (DTT), 18.8 μM EDTA and 1 mg mL^{-1} protease inhibitors (Roche, UK), then centrifuged (21,000 g, 30 min, 4°C). One volume of ice-cold 20% trichloroacetic acid in acetone was added to the supernatant. Proteins were precipitated (-20°C, 1 h) and centrifuged (21,000 g, 15 min, 4°C). The pellet was washed twice in ice-cold acetone using sonication followed by repeat centrifugation. The acetone was discarded and the tube left open at -20°C for 10 min. The pellet was sonicated in 200 μL of ice-cold C1 buffer, containing 6 M urea, 1.5 M thiourea, 3% 3-[(3-cholamidopropyl) dimethylammonio]-1-propanesulfonate (CHAPS), 66 mM DTT, and 0.5% Pharmalyte pH 3-10 (GE Healthcare, UK), then centrifuged (13,000 g, 5 s). Protein in the supernatant was assayed using Bradford reagent (Sigma, UK).

Two-dimensional gel electrophoresis (2-DE)

Protein samples (100 ng) in 125 μL C1 buffer were soaked overnight into 7 cm pH 3-10 NL IPG strips (Bio-Rad, UK). Isoelectrofocusing was performed at 4000 V to a total of 10,000 Vh in a Protean IEF Cell (Bio-Rad, UK). Strips were then equilibrated for 15 min in bromophenol blue-dyed buffer (50 mM Tris-Cl pH 8.8, 6 M urea, 30% v/v glycerol, 2% w/v SDS, 5 mg mL^{-1} DTT), then another 15 min in buffer with 15 mg mL^{-1} iodoacetamide replacing DTT. Second dimension electrophoresis was performed by the standard Laemmli system on 12.5%

polyacrylamide running gels in a Tetra Gel Electrophoresis tank (Bio-Rad, UK), in 1× TGS buffer (Bio-Rad, UK), for 20 min at 70 V, then at 200 V until the end of dye migration.

The 2-DE gels were stained using Coomassie Phastgel Blue R-250 (GE Healthcare, UK), and their images were scanned on a GS-800 calibrated imaging densitometer (Bio-Rad, UK), and imported into Progenesis PG220 v2006 software (Nonlinear Dynamics, UK). Following automated spot detection, manual editing of boundaries was performed on a single ‘reference’ gel (one of the APC3 triplicates) with the greatest number of visible spots. A few landmark spots were ‘locked’ to match other gels to the reference in Progenesis ‘warping’ mode. Then spot matches were performed manually, using a consistent small threshold. Spot numbers were then automatically synchronized, before background subtraction using the ‘mode of non-spot’ method, and normalization of spot volumes using total spot volume multiplied by total area. Unmatched spots were then reviewed using the ‘difference map’ and, if added, the background subtraction and normalization were repeated.

For the multivariate analysis presented in Results, each gel, regardless of strain or experiment, was matched to the single APC3 reference gel as described above. This was deemed a non-biased strategy for strain discrimination, rather than creating a master gel from averaged gels of each strain. For comparison, the numbers of matched spots per gel using both alternatives are shown in Supplementary Table 1.

Data analysis

Normalized volumes of all spots indexed in the Progenesis software were exported as data files. Spots identified in all three replicates of any strain(s) were collated for multivariate analysis. This yielded a data matrix of 27 (gels) × 619 (spots). Principal component analysis (PCA) was performed on mean-centered, unscaled data in SIMCA-P v.11 software (Umetrics, Sweden). The resultant PCs were employed in canonical variates analysis (CVA) with fungal strains as groups, and permutation analysis of Mahalanobis squared distances (De Maesschalck *et al.* 2000) between any two defined groups, in PAST v.2.17c (Hammer *et al.* 2001). Pearson correlation analysis was also performed in PAST.

Protein sequencing and identification

Plugs (1-2 mm) from protein spots of interest were manually excised from the gel and destained in 50 µL of 50% acetonitrile/50% NH₄HCO₃ for 15 min at 37°C, repeated as necessary. After dehydration (10 µL acetonitrile, 37°C, 30-45 min) plugs were rehydrated

overnight in 9 μ L 50 mM NH_4HCO_3 /1 μ L trypsin (Sigma, UK) at 37°C. Then plugs were twice eluted (30 μ L 60% acetonitrile /1% trifluoroacetic acid with three 2 min sonications and ice-cooling), and the pooled eluates dried in a vacuum centrifuge. The resulting peptides were resuspended in 10 μ L of 5% acetonitrile /0.05% trifluoroacetic acid.

Peptides from digested protein spots were desalted using C18 ZipTips (Millipore, UK) according to the manufacturer's instructions. Samples were loaded into gold coated nano-vials and sprayed under atmospheric pressure at 800-900 V in a Q-ToF-1.5 hybrid mass spectrometer (Waters, UK). From full scan mass spectra, ions were identified as possible tryptic peptides. Tandem (MS/MS) mass spectra, obtained for these ions by collision-induced dissociation (using argon collision gas), were recorded over m/z 80-1400 Da with scan time 1 s. MassLynx v.3.5 ProteinLynx (Waters, UK) was used to process raw fragmentation spectra. Each spectrum was combined and smoothed twice by the Savitzky-Golay method at ± 3 channels, with background noise subtracted at polynomial order 15 and 10% below curve. Monoisotopic peaks were centred at 80% centroid setting. Peak mass lists for each spectrum were exported in .dta format, and spectra common to each 2-DE spot concatenated into a single MASCOT generic format (.mgf) file using the merge.pl Perl script (www.matrixscience.com). Merged files were submitted to a MASCOT MS/MS ions search within a locally installed MASCOT server to search the NCBI nr protein database (16/12/2015). Search parameters were as described in Morpew *et al.* (2012). BLAST searches were used to obtain functional hypotheses for *M. perniciosus* accessions without functional annotation. *M. perniciosus* transcript sequences with similar predicted functions or InterPro domains, and high sequence identity to the MS/MS peptides, were identified among the RNA-seq libraries of the Witches' Broom Disease Transcriptome Atlas (WBDTA) at <http://bioinfo08.ibi.unicamp.br/wbdatlas> (Teixeira *et al.* 2014).

Results and discussion

Developmental characters of *M. pernicios* strains

Differences in saprotrophic growth and morphology between *M. pernicios* isolates were seen during *in vitro* culture on MYEA medium (Fig 1), and remained consistent over four years of observation. The Ecuadorian L-biotype isolate (SCFT) had the most transparent texture, due to mycelia of lower density tending to grow in an aerial manner. At the other extreme was the Bolivian C-biotype YB2, which produced snow-white colonies with dense, entangled hyphae anchored to the medium, and little aerial mycelium. The other isolates showed intermediate hyphal densities and propensities to aerial growth, with the geographically diverse C-biotypes RNBP1, Cast1 and GC-A5 forming relatively abundant aerial hyphae. The distinctive mycelia exemplified by SCFT and YB2 were similar to the phenotypes described respectively as ‘flocculent’ and ‘compact’ by Alvim *et al.* (2009), who observed either in the genome-sequenced *M. pernicios* isolate FA553, depending on carbon source. Further details of colony morphologies are in Supplementary Table 2.

We found that colony expansion rates varied considerably between isolates (Fig 1). The dense colonies of YB2 were extremely slow-growing (1.0 mm d^{-1} between days 9-13 of culture). The fastest growth was exhibited by the Brazilian S-biotype APS1 (3.2 mm d^{-1}). Among C-biotypes, the Brazilian Cast1 grew fastest (2.7 mm d^{-1}), followed by APC3, PichiE and RNBP1 ($2.4\text{-}2.5 \text{ mm d}^{-1}$). Relatively slow-growing isolates were the Trinidadian C-biotype GC-A5 (2.0 mm d^{-1}), and the Brazilian S-biotype WMA5 (1.9 mm d^{-1}).

Comparative virulence of C- and S-biotypes

We sought to confirm the host specificities of S- and C-biotype strains using plant infections. Infective spores of the S-biotype isolates (WMA5 and APS1), and of the APC3 and Cast1 C-biotypes were obtained from *ex planta* basidiomes by the method of Griffith and Hedger (1993). Mist conditions were used to induce fructification in dense white mycelial cultures on a bran-vermiculite matrix, resulting in crimson pigmentation of the mycelial surface within two days, and patches of basidiome primordia after about ten days. Differences in fructification dynamics and basidiome characters were evident between the four strains. Fructification was rapid and abundant in WMA5, which yielded up to 150 basidiomes per dish by the fifth day post-induction. In contrast, APS1 and APC3 produced ten-fold fewer basidiomes at a time,

over longer periods. Cast1 fructification varied from sparse to coverage of half the pie dish surface. Maximum pileus diameter was greatest in APC3 (3.3 cm), and smallest in APS1 (2.2 cm). All four strains displayed a range of pink to crimson pigmentation on pilei, gills and stipes, as shown in Supplementary Fig 1. No basidiome characters specific to either C- or S-biotype were identified.

Spores collected from the *ex planta* basidiomes were used to infect young cacao and tomato plants, respectively putative hosts for the C- and S-biotypes (Fig 2). All cacao plants inoculated with the C-biotype APC3 ($n = 5$) developed stem swelling and axillary shoot proliferation (Fig 2A), characteristic symptoms of witches' broom disease. On cacao inoculated with the S-biotype WMA5 ($n = 5$) or controls ($n = 8$), these symptoms were not observed (Fig 2A). Less predictably, inoculation of tomato with spores of the C-biotype Cast1 induced some stem swelling, fasciation, and flushing of axillary shoots (Fig 2B) on 3 out of 12 plants. Spores of the APC3 C-biotype induced very mild stem swellings and faint stem epidermis necrosis on 5 out of 6 inoculated tomato plants. Tomato plants inoculated with the S-biotype WMA5 ($n = 6$) developed pronounced symptoms, including stunting, stem widening and fasciation, leaf deformations and abnormal axillary shoots.

For a long time, C- and S- biotypes were thought not to cross-infect each others' hosts (Bastos and Evans 1985). Our observations, however, add to more recent findings of C-biotype induced symptoms on a solanaceous host. Lopes *et al.* (2001) found symptoms on both malvaceous (*Theobroma cacao*, *T. bicolor* and *T. grandiflorum*) and solanaceous (*Solanum paniculatum*) hosts upon cross-inoculation with each other's *M. perniciosus* isolates. Deganello *et al.* (2014) observed an 18% height reduction when the Micro-Tom tomato cultivar was inoculated with a C-biotype isolate from Uruçuca, Bahia, though no other morphological symptoms were seen. Defence gene expression kinetics in these C-biotype infections were interpretable as a non-host response (Deganello *et al.* 2014). The same study found that S-biotype disease progression in tomato suggested broken non-host resistance rather than a fully adapted pathogen (Deganello *et al.* 2014).

Proteomic comparison of cultured strains

Strains were compared by 2-DE of proteins extracted from triplicate top-layer cultures on MYEA medium (Fig 1). One APC3 gel was selected (for high spot count) as the reference to which others were matched using Progenesis PG220 software. On average, 364 (SD, 52) spots on each gel were matched to the APC3 reference. To explore whether similarities between

strains might be evident from the 2-DE gels, we performed multivariate data analyses on the spot volume data. We collated only spots present in all replicate gels of at least one strain, on the assumption that these might be most strain-informative.

We first applied PCA to the spot data. As the first two PCs accounted for only 32% of overall variance, pairwise PC scores plots offered limited explanatory power. However, we recruited 68.1% of the data variance by using CVA on the scores of the first eight PCs (Fig 3). CVA derives linear combinations of variables (here, PCs of the 2-DE data) to produce maximal, and second-to-maximal, separation between defined groups (here, fungal strains) on the first two canonical axes.

On the CVA plot (Fig 3), the slow-growing YB2 culture occupied the most negative region of the (vertical) canonical axis 2, while faster growing cultures occupied the positive region. A possible relation between growth properties and proteomes of the cultures was supported by a correlation coefficient of -0.752 ($p < 0.05$) between growth rates and mean values on axis 2 for each strain.

The L-biotype SCFT appeared separate from all other strains on the CVA plot (Fig 3). For statistical support, we used permutation with 2000 pseudoreplicates on the Mahalanobis squared distance (MD^2) between the multivariate data (i.e., scores on eight PCs) for any two defined groups. This non-parametric test confirmed a significant distance between SCFT and the C- and S-biotypes ($MD^2 = 33.36$; $p < 0.01$).

On the other hand, the S-biotypes APS1 and WMA5 did not associate as a distinct group on the CVA plot, being interspersed with the C-biotypes GC-A5 and PichiE (Fig 3). Furthermore, the two-group permutation test did not significantly separate the APS1/WMA5 pair from the other biotypes ($MD^2 = 5.683$; $p = 0.06$). The proteomic similarity of the S- and C-biotypes could be seen as consistent with the DNA evidence that these biotypes are not phylogenetically distinct (de Arruda *et al.* 2005; Marelli *et al.* 2009).

Certain C-biotypes occurred in proximity on the CVA plot (Fig 3). One apparent association was Cast1/APC3, and this pair was significantly separated from all other strains in the permutation test ($MD^2 = 12.61$; $p < 0.01$). Cast1 and APC3 were isolated over a decade apart in different Brazilian states (Table 1), but do share the property of being able to infect the cacao clone Scavina 6, which is resistant to many witches' broom strains, including GC-A5 (Shaw and Vandebon 2007). However, the relative virulence of these strains differs on other cacao clones (Shaw and Vandebon 2007). RNBP1 and YB2 were likewise in proximity on the CVA

plot, and as a pair were significantly separated from all other strains in the permutation test ($MD^2 = 12.50$; $p < 0.01$). RBNP1 and YB2 were, again, isolated over a decade apart, but geographically both came from the Western reaches of the Amazon basin (Table 1).

Identification of proteins of *M. pernicioso* cultures

Information on sufficiently abundant proteins on the APC3 and Cast1 C-biotype gels was obtained by MASCOT searches of databases using MS/MS sequences of tryptic peptides from 2-DE gel spots (Table 2). For most queries, an accession from the genus *Moniliophthora* was the best match. At the time of this study, the *M. pernicioso* genome version deposited at DDBJ/EMBL/GenBank was lower quality (accession ABRE, 1.9× coverage) than that of *M. roreri* (accession LATX, 91× coverage). Consequently, the *M. roreri* genome provided the MASCOT matches in 16 queries, while *M. pernicioso* provided only 11, seven of which were partial sequences (Table 2). For one query (spot 12), the MASCOT match was from another genome-sequenced agaric *Schizophyllum commune* (Ohm *et al.* 2010), but this sequence showed 94% identity to an *M. pernicioso* accession, EEB94528.

Another new resource is the WBDTA, based on RNA-seq libraries of RNAs from a range of cultures and pathogenic stages of *M. pernicioso* (Teixeira *et al.* 2014). NCBI database information (function and InterPro domains) on accessions similar to the 2-DE spots (Table 2) was used further, to identify similar transcripts in the WBDTA. Transcripts (MP identifiers) with high identity to the 2-DE spots peptides are in Table 3. The 14-day-old dikaryotic mycelial cultures library of the WBDTA would be the most comparable to the cultures we analyzed. Table 3 therefore reports expression of the relevant transcripts in this library, as well as the library in which they exhibited maximal expression. Eighteen of the 20 matched genes showed substantial expression in 14-day-old dikaryotic mycelia (over 20% of the maximal expression during the life-cycle), making a relationship to our 2-DE spots plausible (Table 3).

An outstanding feature of the *M. pernicioso* proteomes (Tables 2-3) was the prominence of putative aldo-keto reductases (AKRs). The AKR superfamily has a common structure and reaction mechanism, involving NADPH-dependent oxido-reduction of carbonyl compounds, but it encompasses diverse functional roles across all phyla (Mindnich and Penning 2009). We found an AKR, spot 1, that was among the most abundant proteins in all cultures (Fig 1), irrespective of biotype (see Supplementary Fig 2 for quantitative data). Spot 1 appeared to correlate with culture growth rate (coefficient 0.77, $p < 0.05$), having lowest abundance in the slow-growing YB2 C-biotype, and highest in the fast-growing APS1 S-biotype. Three other

spots were assigned as AKRs (Tables 2-3). Two of these (16, 17) were moderately abundant in all strains, but spot 4 showed great variability (Supplementary Fig 2). Spot 4 was present in all replicates of the C-biotype APC3, but in other strains such as the C-biotype Cast1, it was not detected (Fig 4 inset). The peptide sequences of spot 4 were found in spot 1 (Supplementary Table 3), and each could be matched to an *M. roreri* accession with a theoretical molecular weight (36.4 kDa) and pI (6.2) similar to the gel estimates for spot 1 (35 kDa, pI 6.5). Spot 4 was estimated to have a similar molecular weight (37 kDa) but more basic pI (8.5), suggesting a modified isoform of the same protein.

Such prominence of AKRs has not been widely reported in fungal cultures on complete media. Leal *et al.* (2010) found *M. pernicioso* AKR transcripts were induced in nitrogen-limited liquid cultures, and were expressed in infected cacao tissues. They proposed AKRs belong to a suite of ‘virulence life-style genes’ that enable colonization of the host environment (Leal *et al.* 2010). One virulence-associated AKR is the *AFTS1* gene of *Alternaria alternata*, involved in biosynthesis of a toxin for pathogenicity on strawberry (Ito *et al.* 2004). In cultures of *Ustilago maydis*, expression of the AKR YakC increased in the transition to filamentous growth associated with the pathogenic life-style (Böhmer *et al.* 2007). Other evidence for AKRs in fungal-plant interactions includes the AAD1 aryl-alcohol dehydrogenase of the lignin-degrader *Phanerochaete chrysosporium* (Yang *et al.* 2012), and up-regulation of AKRs in the *Rhizophagus irregularis*-*Medicago truncatula* symbiosis (Tisserant *et al.* 2013). In other fungal systems, AKRs detoxify xenobiotics, such as pharmaceuticals in *Candida glabrata* (Farahyar *et al.* 2013). Evidence also supports a role for fungal AKRs in stress responses. Yeast mutants defective in AKR genes, for example, exhibited abnormal oxidative and heat stress (Chang and Petrash 2008). The putative AKR gene MP13440, which shared high identity with the spots 1, 4 and 17 peptides, had highest expression in infected fruit in the WBDTA (Table 3), but little (< 1% of maximum) in green brooms. The role of AKRs in witches’ broom disease awaits elucidation.

Several other proteins in our cultures would be consistent with a stress response syndrome (Tables 2-3). These included two heat-shock proteins found in all strains (spots 11 and 12). In addition, a 1-cys peroxiredoxin (spot 6) was detected on most gels, generally in high amounts in the faster-growing strains, but showed considerable variability even between replicates (Supplementary Fig 2). Peroxiredoxins are widely distributed peroxide-decomposing enzymes (Monteiro *et al.* 2007). Cobos *et al.* (2010) detected peroxiredoxin, and heat-shock protein, in

liquid cultures of the grapevine pathogen *Diplodia seriata*, and speculated that peroxiredoxin could contribute to pathogenesis by counteracting host-produced hydrogen peroxide.

Spot 18 had a negative correlation with growth rate (coefficient -0.78, $p < 0.05$), being found in greatest abundance in the slow-growing YB2 cultures (Supplementary Fig 2). It showed homology to mannitol-1-phosphate dehydrogenase (Tables 2-3), which functions in biosynthesis of mannitol, a compatible solute produced by fungi in response to various stresses (Dijksterhuis and De Vries 2006). Interestingly, mannitol-1-phosphate dehydrogenase appears to have been acquired by the *Moniliophthora* genus via horizontal gene transfer from firmicute bacteria (Tiburcio *et al.* 2010). These authors point out that *Moniliophthora* relatives are saprotrophs (Aime and Phillips-Mora 2005), so a pre-pathogenic ancestor might have occupied soil and decomposed organic material, in which firmicutes are common. Acquisition of mannitol-1-phosphate dehydrogenase by a *Moniliophthora* ancestor might have contributed to the evolution of pathogenicity. *Alternaria alternata* mutants in this enzyme, for example, were less virulent on tobacco (Vélèz *et al.* 2008). Ascomycetes such as *Alternaria*, however, appear to have acquired mannitol-1-phosphate dehydrogenase by a different horizontal gene transfer, from actinobacteria (Tiburcio *et al.* 2010). In contrast, most basidiomycetes other than *Moniliophthora* appear to lack mannitol-1-phosphate dehydrogenase, which Tiburcio *et al.* (2010) speculate is one reason why there are more phytopathogens among ascomycetes than basidiomycetes. This protein is therefore a further possible ‘virulence life-style’ function in the cultured *M. perniciosa* proteome.

About one-third of the gel spots in Tables 2-3 were assignable to central metabolism enzymes generally encountered in fungal proteomic studies. Malate dehydrogenase (spots 2 and 14), phosphoglycerate kinase (spot 3), and glyceraldehyde-3-phosphate dehydrogenase (spots 10 and 20) featured in proteomic analyses of cultures of *M. perniciosa* (Silva *et al.* 2013), other agaricomycetes such as *Rhizoctonia solani* (Kwon *et al.* 2014) and *Phanerochaete chrysosporium* (Yildirim *et al.* 2014), and ascomycetes including *Diplodia seriata* (Cobos *et al.* 2010) and *Aspergillus fumigatus* (Vödisch *et al.* 2009). Since *M. perniciosa* has been found to possess only one glyceraldehyde-3-phosphate dehydrogenase gene (Lima *et al.*, 2009), spot 20 was likely a modified version of spot 10, with a similar molecular weight, but slightly less basic pI (Fig 4). Two isoforms with similar molecular weight and pI were also found in the pathogenic ascomycete *Paracoccidioides brasiliensis* (Barbosa *et al.*, 2006).

For each of these ubiquitous enzymes, specialized extra functions have been proposed. Glyceraldehyde-3-phosphate dehydrogenase has been identified as a virulence factor in

mycoses caused by *Candida albicans* and *Paracoccidioides brasiliensis* (Barbosa *et al.* 2006; Seidler 2013). The other glycolytic enzymes enolase (spot 13) and phosphoglycerate kinase have also been implicated in mycoses (Pancholi and Chhatwal 2003). Malate dehydrogenase may be indirectly involved in virulence in *M. pernicioso*. Oxaloacetate produced by this enzyme may be converted into oxalate, from which *M. pernicioso* can make calcium oxalate, which appears to play a role in pathogenesis (Ceita *et al.* 2007; do Rio *et al.* 2008). The genes MP02237, MP03476, MP05722, MP05723, MP12535 with similar sequences to these carbohydrate metabolism enzymes (Table 3) all had strong expression in the WBDTA green broom libraries (252-1955 RPKM).

Spot 9 was matched to *M. pernicioso* accession EEB89936 (hypothetical protein MPER_11918), which had 61% homology with the *Pleurotus ostreatus* protein pleurotolysin B, of the membrane pore-forming aegerolysin family (Tomita *et al.* 2004). The discrepancy between theoretical (57.2 kDa) and observed (41 kDa) molecular weights of this protein was consistent with the reported proteolytic cleavage in *P. ostreatus* extracts of the 59 kDa pleurotolysin B into a 41 kDa fragment (Tomita *et al.* 2004). Using an *M. pernicioso* culture system based on Griffith and Hedger (1993), Pires *et al.* (2009) found differential expression of aegerolysin transcripts during fructification, and have already associated MPER_11918 with the probable pleurotolysin B of *M. pernicioso*. A role for aegerolysins in the later stages of development would be consistent with the fact that we only observed spot 9 in the fast-growing Cast1 cultures (Fig 4), whose mycelia may have been in a more advanced developmental state (though basidiome formation was observed in these cultures and has not been reported from any Petri dish cultures). The WBDTA gene most similar to spot 9, MP13610, had strongest expression in basidiome primordia and little in mycelial cultures (Table 3). Similar comments apply to the putative NAD-dependent epimerase spot 5 (Fig 4), of unknown function, and its most similar WBDTA gene MP04655 (Table 3).

Other library matches of potential relevance to pathogenesis included a putative nitrilase (spot 15), a function highlighted in the *M. pernicioso* genome by Mondego *et al.* (2008) as an auxin biosynthesis step, via hydrolysis of indole-3-acetonitrile. Alternatively, nitrilase could detoxify plant-produced cyanides (O'Reilly and Turner 2003). Spot 21 was identified as an NAD-dependent formate dehydrogenase, which in *M. pernicioso* may have a role in catabolism of methanol released by hydrolysis of methylesterified host pectins (Mondego *et al.* 2008; De Oliveira *et al.* 2012).

It should be stated that the subset of proteins identified by MS/MS were self-selected for

sufficient abundance on the gels. The sequenced protein spots in Supplementary Fig 2 contributed 12.9% of the total variance explored by CVA (Fig 3). Consequently, the proteomic phenotypes indicated by CVA will remain ‘black boxes’ until a more comprehensive characterization of the protein populations. Nonetheless this study supports the potential of multivariate analysis and sequence informatics for understanding fungal proteomes.

Conclusions

Cultures of geographically diverse *M. pernicios* isolates exhibited differences in mycelial and basidiome morphology, and also in rates of saprotrophic growth and fructification, but no biotype-specific characters were observable. In infection experiments, moreover, one of the C-biotypes caused symptoms on tomato, a putative S-biotype host. The lack of a clear distinction between C- and S-biotypes also applied at the proteome level, as multivariate analyses of 2-DE spot patterns did not discriminate these two biotypes. These observations accord with genetic studies that failed to separate C- and S-biotypes (De Arruda *et al.* 2005; Marelli *et al.* 2009). The single L-biotype, however, was statistically different in our proteomic analyses.

Peptide sequencing of 2-DE spots from *M. pernicios* cultures confirmed the utility of recent genome sequencing, including *M. roreri*, which contributed a number of functional annotations. The proteome of *in vitro* cultured *M. pernicios* was suggestive of the ‘virulence life-style’ proposed on the basis of transcript analyses by Leal *et al.* (2010). Unlike these authors, we did not subject the saprotrophic cultures to any treatment designed to mimic a host environment and yet, interestingly, the sampled proteome presented a high proportion of functions indicative of pathogenicity.

Acknowledgements

We dedicate this paper to the memory of Dr. Sandra Pierre who died in March 2017. She had a huge enthusiasm for cocoa research and will be greatly missed by her former colleagues.

This work was funded by Cocoa Research UK Ltd and the Government of the Netherlands. We are grateful for technical assistance and advice from James Heald, Martyna Matuszyk, Sarah Tvedt, Jon Lamb, Martin Swain, Tom Thomas, Pat Causton, Anthony Pugh, Gwen Jenkins and Joanne Hamilton.

Appendix A. Supplementary data

Supplementary data associated with this article can be found, in the online version, at

REFERENCES

- Aime MC, Phillips-Mora W, 2005. The causal agents of witches' broom and frosty pod rot of cacao (chocolate, *Theobroma cacao*) form a new lineage of Marasmiaceae. *Mycologia* **97**: 1012-1022.
- Alvim FC, Mattos EM, Pirovani CP, Gramacho K, Pungartnik C, Brendel M, Cascardo JCM, Vincentz M, 2009. Carbon source-induced changes in the physiology of the cacao pathogen *Moniliophthora perniciosa* (Basidiomycetes) affect mycelial morphology and secretion of necrosis-inducing proteins. *Genetics and Molecular Research* **8**: 1035-1050.
- Barbosa MS, Bão SN, Andreotti PF, Faria FP, Felipe MSS, Feitosa LS, Mendes-Giannini MJS, Soares CMA, 2006. Glyceraldehyde-3-phosphate dehydrogenase of *Paracoccidioides brasiliensis* is a cell surface protein involved in fungal adhesion to extracellular matrix proteins and interaction with cells. *Infection and Immunity* **74**: 382-389.
- Bastos CN, Evans HC, 1985. A new pathotype of *Crinipellis perniciosa* (witches' broom disease) on solanaceous hosts. *Plant Pathology* **34**: 306-312.
- Böhmer M, Colby T, Böhmer C, Bräutigam A, Schmidt J, Bölker M, 2007. Proteomic analysis of dimorphic transition in the phytopathogenic fungus *Ustilago maydis*. *Proteomics* **7**: 675-685.
- Ceita GDO, Macedo JNA, Santos TB, Alemanno L, Gesteira AD, Micheli F, Mariano AC, Gramacho KP, Silva DDC, Meinhardt L, Mazzafera P, Pereira GAG, Cascardo J, 2007. Involvement of calcium oxalate degradation during programmed cell death in *Theobroma cacao* tissues triggered by the hemibiotrophic fungus *Moniliophthora perniciosa*. *Plant Science* **173**: 106-117.
- Chang Q, Petrash JM, 2008. Disruption of aldo-keto reductase genes leads to elevated markers of oxidative stress and inositol auxotrophy in *Saccharomyces cerevisiae*. *Biochimica et Biophysica Acta* **1783**: 237-245.
- Cobos R, Barreiro C, Mateos RM, Coque JJR, 2010. Cytoplasmic- and extracellular-proteome analysis of *Diplodia seriata*: a phytopathogenic fungus involved in grapevine decline. *Proteome Science* **8**: 46.

- Cohen BL, 1973. Growth of *Apergillus nidulans* in a thin liquid layer. *Microbiology* **76**: 277-282.
- De Arruda MCC, Sepulveda Ch. GF, Miller RNG, Ferreira MASV, Santiago DVR, Resende MLV, Dianese JC, Felipe MSS, 2005. *Crinipellis brasiliensis*, a new species based on morphological and molecular data. *Mycologia* **97**: 1348-1361.
- Deganello J, Leal GA, Rossi ML, Peres LEP, Figueira A, 2014. Interaction of *Moniliophthora perniciosa* biotypes with Micro-Tom tomato: a model system to investigate the witches' broom disease of *Theobroma cacao*. *Plant Pathology* **63**: 1251-1263.
- De Maesschalck R, Jouan-Rimbaud D, Massart DL, 2000. The Mahalanobis distance. *Chemometrics and Intelligent Laboratory Systems* **50**: 1-18.
- De Oliveira BV, Teixeira GS, Reis O, Barau JG, Teixeira PJPL, do Rio MCS, Domingues RR, Meinhardt LW, Paes Leme AF, Rincones J, Pereira GAG, 2012. A potential role for an extracellular methanol oxidase secreted by *Moniliophthora perniciosa* in Witches' broom disease in cacao. *Fungal Genetics and Biology* **49**: 922-932.
- Díaz-Valderrama JR, Aime MC, 2016. The cacao pathogen *Moniliophthora roreri* (Marasmiaceae) possesses biallelic *A* and *B* mating loci but reproduces clonally. *Heredity* **116**: 491-501.
- Dijksterhuis J, De Vries RP, 2006. Compatible solutes and fungal development. *Biochemical Journal* **399**: e3-e5.
- Do Rio MCS, de Oliveira BV, de Tomazella DPT, Silva JAF, Pereira GAG, 2008. Production of calcium oxalate crystals by the Basidiomycete *Moniliophthora perniciosa*, the causal agent of witches' broom disease of cacao. *Current Microbiology* **56**: 363-370.
- Farahyar S, Zaini F, Kordbacheh P, Rezaie S, Safara M, Raoofian R, Heidari M, 2013. Overexpression of aldo-keto-reductase in azole-resistant clinical isolates of *Candida glabrata* determined by cDNA-AFLP. *DARU Journal of Pharmaceutical Sciences* **21**:1.
- Fernández-Acero FJ, Jorge I, Calvo E, Vallejo I, Carbú M, Camafeita E, Garrido C, López JA, Jorrín J, Cantoral JM, 2007. Proteomic analysis of phytopathogenic fungus *Botrytis cinerea* as a potential tool for identifying pathogenicity factors, therapeutic targets and for basic research. *Archives of Microbiology* **187**: 207-215.

- Fernández-Acero FJ, Jorge I, Calvo E, Vallejo I, Carbú M, Camafeita E, López JA, Cantoral JM, Jorrín J, 2006. Two-dimensional electrophoresis protein profile of the phytopathogenic fungus *Botrytis cinerea*. *Proteomics* **6**: S88-S96.
- Franco SF, Baroni RM, Carazzolle MF, Teixeira PJPL, Reis O, Pereira GAG, Mondego JMC, 2015. Genomic analyses and expression evaluation of thaumatin-like gene family in the cacao fungal pathogen *Moniliophthora perniciosa*. *Biochemical and Biophysical Research Communications* **466**: 629-636.
- Gomes DS, Lopes MA, Menezes SP, Ribeiro LF, Dias CV, Andrade BS, de Jesus RM, Pires ABL, Goes-Neto A, Micheli F, 2016. Mycelial development preceding basidioma formation in *Moniliophthora perniciosa* is associated to chitin, sugar and nutrient metabolism alterations involving autophagy. *Fungal Genetics and Biology* **86**: 33-46.
- Griffith GW, Hedger JN, 1993. A novel method for producing basidiocarps of the cocoa pathogen *Crinipellis perniciosa* using a bran-vermiculite medium. *Netherlands Journal of Plant Pathology* **99**: 227-230.
- Griffith GW, Hedger JN, 1994a. The breeding biology of biotypes of the witches' broom pathogen of cocoa, *Crinipellis perniciosa*. *Heredity* **72**: 278-289.
- Griffith GW, Hedger JN, 1994b. Spatial distribution of mycelia of the liana (L-) biotype of the agaric *Crinipellis perniciosa* (Stahel) Singer in tropical forest. *New Phytologist* **127**: 243-259.
- Griffith GW, Nicholson JN, Nenninger A, Birch RN, Hedger JN, 2003. Witches' brooms and frosty pods: two major pathogens of cacao. *New Zealand Journal of Botany* **41**: 423-435.
- Hammer Ø, Harper DAT, Ryan PD, 2001. PAST: paleontological statistics software package for education and data analysis. *Palaeontologia Electronica* **4**(1): 9pp.
- Ito K, Tanaka T, Hatta R, Yamamoto M, Akimitsu K, Tsuge T, 2004. Dissection of the host range of the fungal plant pathogen *Alternaria alternata* by modification of secondary metabolism. *Molecular Microbiology* **52**: 399-411.
- Kwon YS, Kim SG, Chung WS, Bae H, Jeong SW, Shin SC, Jeong MJ, Park SC, Kwak YS, Bae DW, Lee YB, 2014. Proteomic analysis of *Rhizoctonia solani* AG-1 sclerotia maturation. *Fungal Biology* **118**: 433-443.
- Leal GA, Gomes LH, Albuquerque PSB, Tavares FCA, Figueira A, 2010. Searching for *Moniliophthora perniciosa* pathogenicity genes. *Fungal Biology* **114**: 842-854.

- 570 Lima JO, Pereira JF, Rincones J, Barau JG, Araujo EF, Pereira GAG, Queiroz MV, 2009. The
571 glyceraldehyde-3-phosphate dehydrogenase gene of *Moniliophthora perniciosa*, the causal
572 agent of witches' broom disease of *Theobroma cacao*. *Genetics and Molecular Biology* **32**:
573 362-366.
- 574 Lopes JRM, Luz EDMN, Bezerra JL, 2001. Suscetibilidade do cupuaçuzeiro e outras espécies
575 vegetais a isolados de *Crinipellis perniciosa* obtidos de quatro hospedeiros diferentes no sul
576 da Bahia. *Fitopatologia Brasileira* **26**: 601-605.
- 577 Mackey AJ, Haystead TAJ, Pearson WR, 2002. Getting more from less. Algorithms for rapid
578 protein identification with multiple short peptide sequences. *Molecular and Cellular*
579 *Proteomics* **1**: 139-147.
- 580 Marelli JP, Maximova SN, Gramacho KP, Kang S, Gultinan MJ, 2009. Infection biology of
581 *Moniliophthora perniciosa* on *Theobroma cacao* and alternate solanaceous hosts. *Tropical*
582 *Plant Biology* **2**: 149-160.
- 583 Meinhardt LW, Bellato CD, Rincones J, Azevedo RA, Cascardo JCM, Pereira GAG, 2006. *In*
584 *vitro* production of biotrophic-like cultures of *Crinipellis perniciosa*, the causal agent of
585 witches' broom disease of *Theobroma cacao*. *Current Microbiology* **52**: 191-196.
- 586 Meinhardt LW, Costa GGL, Thomazella DPT, Teixeira PJPL, Carazzolle MF, Schuster SC,
587 Carlson JE, Gultinan MJ, Mieczkowski P, Farmer A, Ramaraj T, Crozier J, Davis RE, Shao
588 J, Melnick RL, Pereira GAG, Bailey BA, 2014. Genome and secretome analysis of the
589 hemibiotrophic fungal pathogen, *Moniliophthora roreri*, which causes frosty pod rot disease
590 of cacao: mechanisms of the biotrophic and necrotrophic phases. *BMC Genomics* **15**: 164.
- 591 Meinhardt LW, Rincones J, Bailey BA, Aime MC, Griffith GW, Zhang D, Pereira GAG, 2008.
592 *Moniliophthora perniciosa*, the causal agent of witches' broom disease of cacao: what's
593 new from this old foe? *Molecular Plant Pathology* **9**: 577-588.
- 594 Mindnich RD, Penning TM, 2009. Aldo-keto reductase (AKR) superfamily: Genomics and
595 annotation. *Human Genomics* **3**: 362-370.
- 596 Mondego JM, Carazzolle MF, Costa GG, Formighieri EF, Parizzi LP, Rincones J, Cotomacci
597 C, Carraro DM, Cunha AF, Carrer H, Vidal RO, Estrela RC, García O, Thomazella DP, de
598 Oliveira BV, Pires AB, Rio MC, Araújo MR, de Moraes MH, Castro LA, Gramacho
599 KP, Gonçalves MS, Neto JP, Neto AG, Barbosa LV, Gultinan MJ, Bailey BA, Meinhardt
600 LW, Cascardo JC, Pereira GA, 2008. A genome survey of *Moniliophthora perniciosa* gives
601 new insights into Witches' Broom Disease of cacao. *BMC Genomics* **9**: 548.

- Monteiro G, Horta BB, Pimenta DC, Augusto O, Netto LES, 2007. Reduction of 1-Cys peroxiredoxins by ascorbate changes the thiol-specific antioxidant paradigm, revealing another function of vitamin C. *Proceedings of the National Academy of Sciences USA* **104**: 4886-4891.
- Morphew RM, Eccleston N, Wilkinson TJ, McGarry J, Perally S, Prescott M, Ward D, Williams D, Paterson S, Raman M, Ravikumar G, Saifullah MK, Abidi SMA, McVeigh P, Maule AG, Brophy PM, LaCourse EJ, 2012. Proteomics and *in silico* approaches to extend understanding of the glutathione transferase superfamily of the tropical liver fluke *Fasciola gigantica*. *Journal of Proteome Research* **11**: 5876-5889.
- Ohm RA, de Jong JF, Lugones LG, Aerts A, Kothe E, Stajich JE, de Vries RP, Record E, Levasseur A, Baker SE, Bartholomew KA, Coutinho PM, Erdmann S, Fowler TJ, Gathman AC, Lombard V, Henrissat B, Knabe N, Kües U, Lilly WW, Lindquist E, Lucas S, Magnuson JK, Piumi F, Raudaskoski M, Salamov A, Schmutz J, Schwarze FW, van Kuyk PA, Horton JS, Grigoriev IV, Wösten HAB, 2010. Genome sequence of the model mushroom *Schizophyllum commune*. *Nature Biotechnology* **28**: 957-965.
- O'Reilly C, Turner PD, 2003. The nitrilase family of CN hydrolysing enzymes - a comparative study. *Journal of Applied Microbiology* **95**: 1161-1174.
- Pancholi V, Chhatwal GS, 2003. Housekeeping enzymes as virulence factors for pathogens. *International Journal of Medical Microbiology* **293**: 391-401.
- Pires ABL, Gramacho KP, Silva DC, Góes-Neto A, Silva MM, Muniz-Sobrinho JS, Porto RF, Villela-Dias C, Brendel M, Cascardo JCM, Pereira GAG, 2009. Early development of *Moniliophthora perniciosa* basidiomata and developmentally regulated genes. *BMC Microbiology* **9**: 158.
- Ploetz RC, Schnell RJ, Ying Z, Zheng Q, Olano CT, Motamayor JC, Johnson ES, 2005. Analysis of molecular diversity in *Crinipellis perniciosa* with AFLP markers. *European Journal of Plant Pathology* **11**: 317-326.
- Rincones J, Mazotti GD, Griffith GW, Pomela AW, Figueira A, Queiroz MV, Pereira JF, Azevedo RA, Pereira GAG, Meinhardt LW, 2006. Genetic variability and chromosome-length polymorphisms of the witches' broom pathogen *Crinipellis perniciosa* from various plant hosts in South America. *Mycological Research* **110**: 821-832.

- Schlumberger S, Kristan KC, Ota K, Frangež R, Molgó J, Sepčić K, Benoit E, Maček P, 2014. Permeability characteristics of cell-membrane pores induced by ostreolysin A/pleurotolysin B, binary pore-forming proteins from the oyster mushroom. *FEBS Letters* **588**: 35-40.
- Seidler NW, 2013. GAPDH, as a virulence factor. *Advances in Experimental Medicine and Biology* **985**: 149-178.
- Shaw MW, Vandenbon AE, 2007. A qualitative host-pathogen interaction in the *Theobroma cacao*-*Moniliophthora perniciosa* pathosystem. *Plant Pathology* **56**: 277-285.
- Silva FAC, Pirovani CP, Menezes S, Pungartnik C, Santiago AS, Costa MGC, Micheli F, Gesteira AS, 2013. Proteomic response of *Moniliophthora perniciosa* exposed to pathogenesis-related protein-10 from *Theobroma cacao*. *Genetics and Molecular Research* **12**: 4855-4868.
- Teixeira PJPL, Thomazella DPT, Reis O, do Prado PFV, do Rio MCS, Fiorin GL, José J, Costa GGL, Negri VA, Mondego JMC, Mieczkowski P, Pereira GAG, 2014. High-resolution transcript profiling of the atypical biotrophic interaction between *Theobroma cacao* and the fungal pathogen *Moniliophthora perniciosa*. *The Plant Cell* **26**: 4245-4269.
- Thomazella DPT, Teixeira PJPL, Oliveira HC, Saviani EE, Rincones J, Toni IM, Reis O, Garcia O, Meinhardt LW, Salgado I, Pereira GAG, 2012. The hemibiotrophic cacao pathogen *Moniliophthora perniciosa* depends on a mitochondrial alternative oxidase for biotrophic development. *New Phytologist* **194**: 1025-1034.
- Tiburcio RA, Costa GGL, Carazzolle MF, Mondego JMC, Schuster SC, Carlson JE, Guiltinan MJ, Bailey BA, Mieczkowski P, Meinhardt LW, Pereira GAG, 2010. Genes acquired by horizontal transfer are potentially involved in the evolution of phytopathogenicity in *Moniliophthora perniciosa* and *Moniliophthora roreri*, two of the major pathogens of cacao. *Journal of Molecular Evolution* **70**: 85-97.
- Tisserant E, Malbreil M, Kuo A, Kohler A, Symeonidi A, Balestrini R, Charron P, Duensing N, Freidit Frey N, Gianinazzi-Pearson V, Gilbert LB, Handa Y, Herr JR, Hijri M, Koul R, Kawaguchi M, Krajinski F, Lammers PJ, Masclaux FG, Murat C, Morin E, Ndikumana S, Pagni M, Petitpierre D, Requena N, Rosikiewicz P, Riley R, Saito K, San Clemente H, Shapiro H, van Tuinen D, Bécard G, Bonfante P, Paszkowski U, Y. Shachar-Hill YY, Tuskan GA, Young JPW, Sanders IR, Henrissat B, Rensing SA, Grigoriev IV, Corradi N, Roux C, Martin F, 2013, Genome of an arbuscular mycorrhizal fungus provides insight into

the oldest plant symbiosis. *Proceedings of the National Academy of Sciences USA* **110**: 20117-20122.

Tomita T, Noguchi K, Mimuro H, Ukaji F, Ito K, Sugawara-Tomita N, Hashimoto Y, 2004. Pleurotolysin, a novel sphingomyelin-specific two-component cytolysin from the edible mushroom *Pleurotus ostreatus*, assembles into a transmembrane pore complex. *Journal of Biological Chemistry* **279**: 26975-26982.

Véléz H, Glassbrook NJ, Daub ME, 2008. Mannitol biosynthesis is required for plant pathogenicity by *Alternaria alternata*. *FEMS Microbiology Letters* **285**: 122-129.

Vödisch M, Albrecht D, Lessing F, Schmidt AD, Winkler R, Guthke R, Brakhage AA, Kniemeyer O, 2009. Two-dimensional proteome reference maps for the human pathogenic filamentous fungus *Aspergillus fumigatus*. *Proteomics* **9**: 1407-1415.

Yang DD, François JM, de Billerbeck GM, 2012. Cloning, expression and characterization of an aryl-alcohol dehydrogenase from the white-rot fungus *Phanerochaete chrysosporium* strain BKM-F-1767. *BMC Microbiology* **12**: 126.

Yildirim V, Özcan S, Becher D, Büttner K, Hecker M, Özcengiz G, 2011. Characterization of proteome alterations in *Phanerochaete chrysosporium* in response to lead exposure. *Proteome Science* **9**: 12.

Table 1 - Provenance of *M. pernicioso* cultures.

Strain	Biotype	Origin	Host if recorded	Date	Collector ^a	CBS Accession No.
APC3	C	Almirante, Bahia, Brazil	Scavina 6 cocoa pod	Late 1990's	AP	CBS 142684
Cast1	C	Castanhal, Rondônia, Brazil	Cocoa tree in area of Scavina 6 resistance breakdown	Early 1980's	BJW	CBS 142685
GC-A5	C	Gran Couva, Trinidad	Dead cocoa broom	Early 1980's	BJW	CBS 142682
PichiE	C	Pichilingue, Ecuador	Dead cocoa broom	Early 1980's	BJW	CBS 142683
RNBP1	C	Quillabamba, Peru	Dead cocoa broom	June 1998	JNH	CBS 142680
YB2	C	Japacani, Bolivia	Dead cocoa broom	June 1987	EAWB	CBS 142679
APS1	S	Minas Gerais, Viçosa, Brazil	Living <i>Lobeira</i> branch	Late 1990's	AP	CBS 142681
WMA5	S	Manaus, Amazonas, Brazil	<i>Solanum rugosum</i>	Jan. 1991	FJW	CBS 142677
SCFT	L	San Carlos, Napo, Ecuador	Liana (<i>Arrabidaea</i> sp.)	1987	GWG	CBS 142678

^a A. Pomella (AP); BJ Wheeler (BJW); JN Hedger (JNH); EA Wyrley-Birch (EAWB); FJ Wilson (FJW); GW Griffith (GWG).

Table 2 Identifications of *M. pernicios* mycelial proteins using MS/MS.

Spot	MASCOT score ^a	Unique peptides ^b	Predicted function	Accession (species)
1	319	5/5	Aldo-keto reductase ^c	XP_007856327 (<i>M. roreri</i>)
	283	4/4	Aldo-keto reductase ^d	EEB99046 (<i>M. pernicios</i>)
2	352	5/5	Malate dehydrogenase ^d	EEB94126 (<i>M. pernicios</i>)
3	321	6/6	Phosphoglycerate kinase ^d	EEB89461 (<i>M. pernicios</i>)
4	195	3/3	Aldo-keto reductase ^c	ESK84368 (<i>M. roreri</i>)
5	470	7/8	NAD-dependent epimerase/dehydratase ^c	XP_007844083 (<i>M. roreri</i>)
6	422	6/8	1-Cys peroxiredoxin ^c	XP_007845258 (<i>M. roreri</i>)
	355	6/7	1-Cys peroxiredoxin ^d	EEB97022 (<i>M. pernicios</i>)
7	257	4/5	Acetyl-acetyltransferase ^c	XP_007843079 (<i>M. roreri</i>)
8	263	5/5	Aspartate aminotransferase ^c	XP_007843679 (<i>M. roreri</i>)
9	235	3/3	Pleurotolysin B homologue ^d	EEB89936 (<i>M. pernicios</i>)
	53	1/1	Erylsin B ^c	XP_007849236 (<i>M. roreri</i>)
10	335	4/5	Glyceraldehyde-3-phosphate dehydrogenase ^d	EEB90046 (<i>M. pernicios</i>)
	267	3/4	Glyceraldehyde-3-phosphate dehydrogenase ^c	XP_007846800 (<i>M. roreri</i>)
11	339	5/5	Heat-shock protein hss1 ^c	XP_007847698 (<i>M. roreri</i>)
12	101	2/3	Heat shock protein sks2 ^d	XP_003035960 (<i>S. commune</i>)
13	193	2/2	Enolase ^c	XP_007847255 (<i>M. roreri</i>)
14	484	6/6	Malate dehydrogenase ^d	EEB96289 (<i>M. pernicios</i>)
	475	7/7	Malate dehydrogenase ^c	XP_007846805 (<i>M. roreri</i>)
15	344	5/5	Nitrilase ^c	XP_007842695 (<i>M. roreri</i>)
16	148	2/3	Aldo-keto reductase ^c	XP_007854364 (<i>M. roreri</i>)
	134	2/3	Aldo-keto reductase ^d	EEB98988 (<i>M. pernicios</i>)
17	69	1/2	Aldo-keto reductase ^d	EEB97935 (<i>M. pernicios</i>)
18	142	3/3	Mannitol-1-phosphate dehydrogenase ^c	XP_007855888 (<i>M. roreri</i>)
19	318	4/4	MPER_00772 (unknown function)	EEB99535 (<i>M. pernicios</i>)
20	144	3/3	Glyceraldehyde-3-phosphate dehydrogenase ^c	XP_007846800 (<i>M. roreri</i>)
21	290	5/5	NAD-dependent formate dehydrogenase ^c	AFO55209 (<i>M. pernicios</i>)
22	86	2/2	Putative anhydrolase ^d	XP_007855443 (<i>M. roreri</i>)

^a MASCOT scores over 68 were considered significant ($p < 0.05$).^b Peptide sequences are in Supplementary Table 3.

692 ^c Function assignment as database accession.

693 ^d Function prediction from BLAST search.

ACCEPTED MANUSCRIPT

ACCEPTED MANUSCRIPT

Table 3 Comparison of *M. perniciosa* mycelial proteins (Table 2) with transcript sequences in the Witches' Broom Disease Transcriptome Atlas (WBDTA).

Spot	Query/database sequence overlap		Gene ID ^a	Predicted function	Expression in WBDTA RNA-Seq libraries (Teixeira <i>et al.</i> 2014)	
	Amino acids	Identity (%)			14-day-old dikaryotic mycelia (RPKM) ^b	Peak expression in life-cycle (RPKM) ^b
1	90	100	MP13440	Aldo-keto reductase	668	Infected young fruit shell (2427)
2	61	100	MP12535	Malate dehydrogenase	462	Non-germinating spores (742)
3	69	100	MP02237	Phosphoglycerate kinase	321	Green broom (469)
4	32	100	MP13440	Aldo-keto reductase	668	Infected young fruit shell (2427)
5	99	100	MP04655	NAD-dependent epimerase/dehydratase	10	Basidiocarps (1662)
6	116	100	MP16197	1-Cys peroxiredoxin	736	7-day-old dikaryotic mycelia (3303)
7	48	100	MP01795	Acetyl-acetyltransferase	701	Young dikaryotic mycelia (807)
8	56	100	MP00138	Aspartate aminotransferase	547	Germinating spores (608)
9	46	100	MP13610	Pleurotolysin B homologue	29	Basidiocarp primordia (2578)
10	67	100	MP05723	Glyceraldehyde-3-phosphate dehydrogenase	11600	Senescent dikaryotic mycelium (23464)
11	58	100	MP00096	Heat-shock protein hss1	1290	Infected necrotic fruit shell (5313)
12	24	100	MP00146	Heat shock protein sks2	224	Basidiocarp primordia (980)
13	31	100	MP03476	Enolase	441	Green broom (1005)
14	136	99.3	MP05722	Malate dehydrogenase	869	Green broom (1955)
15	79	100	MP00452	Nitrilase	882	Senescent dikaryotic mycelium (1166)
16	38	100	MP12009	Aldo-keto reductase	200	Young dikaryotic mycelium (473)
17	12	92-100 ^c	MP13440	Aldo-keto reductase	668	Infected young fruit shell (2427)
18	30	100	MP10747	Mannitol-1-phosphate dehydrogenase	6897	14-day-old dikaryotic mycelia (6897)
19	-	-				
20	42	100	MP05723	Glyceraldehyde-3-phosphate dehydrogenase	11600	Senescent dikaryotic mycelium (23464)
21	55	100	MP03866	NAD-dependent formate dehydrogenase	2872	28-day-old dikaryotic mycelia (4213)
22	-	-				

^a Identifiers of the WBDTA (<http://bioinfo08.ibi.unicamp.br/wbdatlas>). ^b RPKM, reads per kilobase per million mapped reads.

^c Polymorphic peptide: YLQENVGAGSIK (in MP13440) and YLKENVGAGSIK (in EEB97935, Table 2), which MS/MS was not able to distinguish.

Fig 1 - Mycelia of *M. pernicios* strains cultured on MYEA (12 d, 25°C) in 9 cm Petri dishes. C-biotypes: Cast1, APC3, RNBP1, YB2, PichiE, GC-A5; S-biotypes: WMA5, APS1; L-biotype: SCFT. Below: 2-DE gel of each strain (arrow locates spot 1 for orientation). Proteins were separated by pH 3-10 on 12.5% SDS-PAGE and stained with Coomassie Phastgel Blue R-250.

Fig 2 - Plants inoculated with *M. pernicios* basidiospores (defoliated to show symptoms). (A) Cacao four weeks after mock-inoculation (control), C-biotype infection (APC3) or S-biotype infection (WMA5). (B) Tomato three weeks post-inoculation with the C-biotype Cast1, exhibiting stem fasciation (left), stem swelling (centre) and shoot proliferation (right). Inset shows uninoculated control stem.

Fig 3 - Canonical variates analysis of eight PCs (68.1% of data variance) from PCA of 619 gel spots (as normalized volumes) on 27 gels. The nine fungal strains were the defined groups. Convex hulls joining data points from biological triplicate gels are labeled by strain.

Fig 4 - 2-DE gel of proteins from cultured *M. pernicios* strain APC3. Samples (100 ng) were subjected to isoelectric focusing in a non-linear IPG strip (7 cm, pH 3-10), then 12.5% SDS-polyacrylamide gel electrophoresis as second dimension. Proteins were stained with Coomassie Phastgel Blue R-250. Arrows indicate peptide-sequenced spots, numbered as in Tables 2-3. Inset shows part of a gel of strain Cast1 corresponding to the rectangle in the APC3 main image.

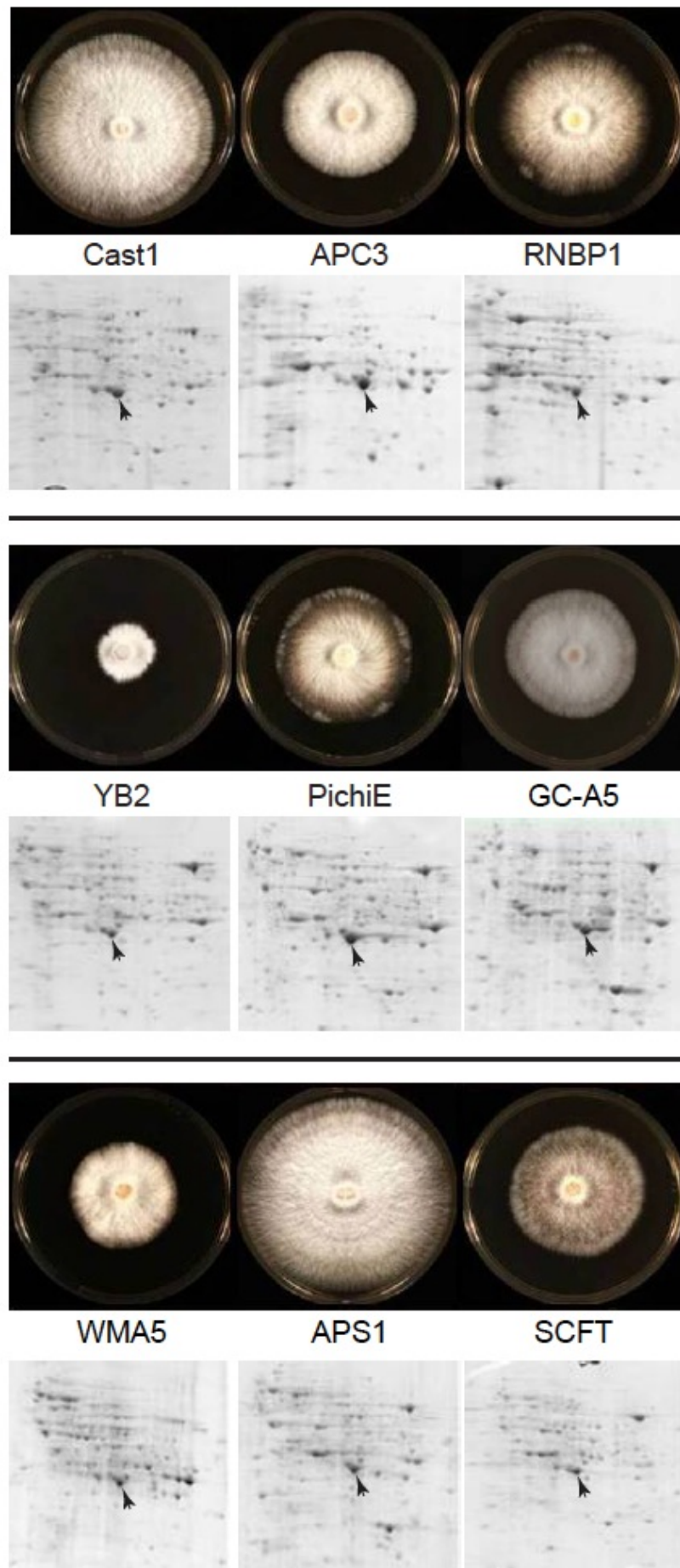


Fig 1 - Mycelia of *M. pernicioso* strains cultured on MYEA (12 d, 25°C) in 9 cm Petri dishes. C-biotypes: Cast1, APC3, RNBp1, YB2, PichiE, GC-A5; S-biotypes: WMA5, APS1; L-biotype: SCFT. Below: 2-DE gel of each strain (arrow locates spot 1 for orientation). Proteins were separated by pH 3-10 on 12.5% SDS-PAGE and stained with Coomassie Phastgel Blue R-250.

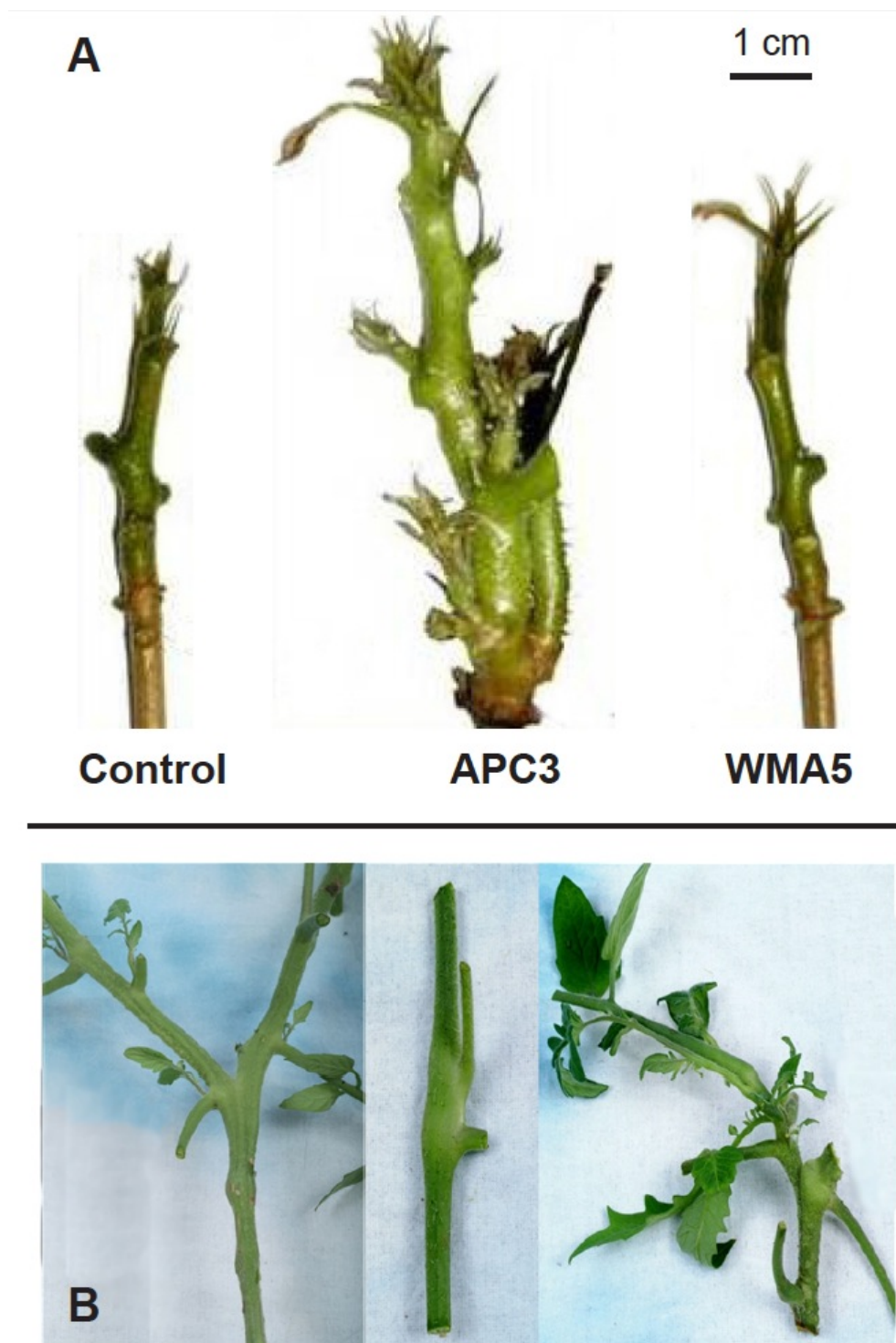


Fig 2 - Plants inoculated with *M. perniciosa* basidiospores (defoliated to show symptoms). (A) Cacao four weeks after mock-inoculation (control), C-biotype infection (APC3) or S-biotype infection (WMA5). (B) Tomato three weeks post-inoculation with the C-biotype Cast1, exhibiting stem fasciation (left), stem swelling (centre) and shoot proliferation (right).

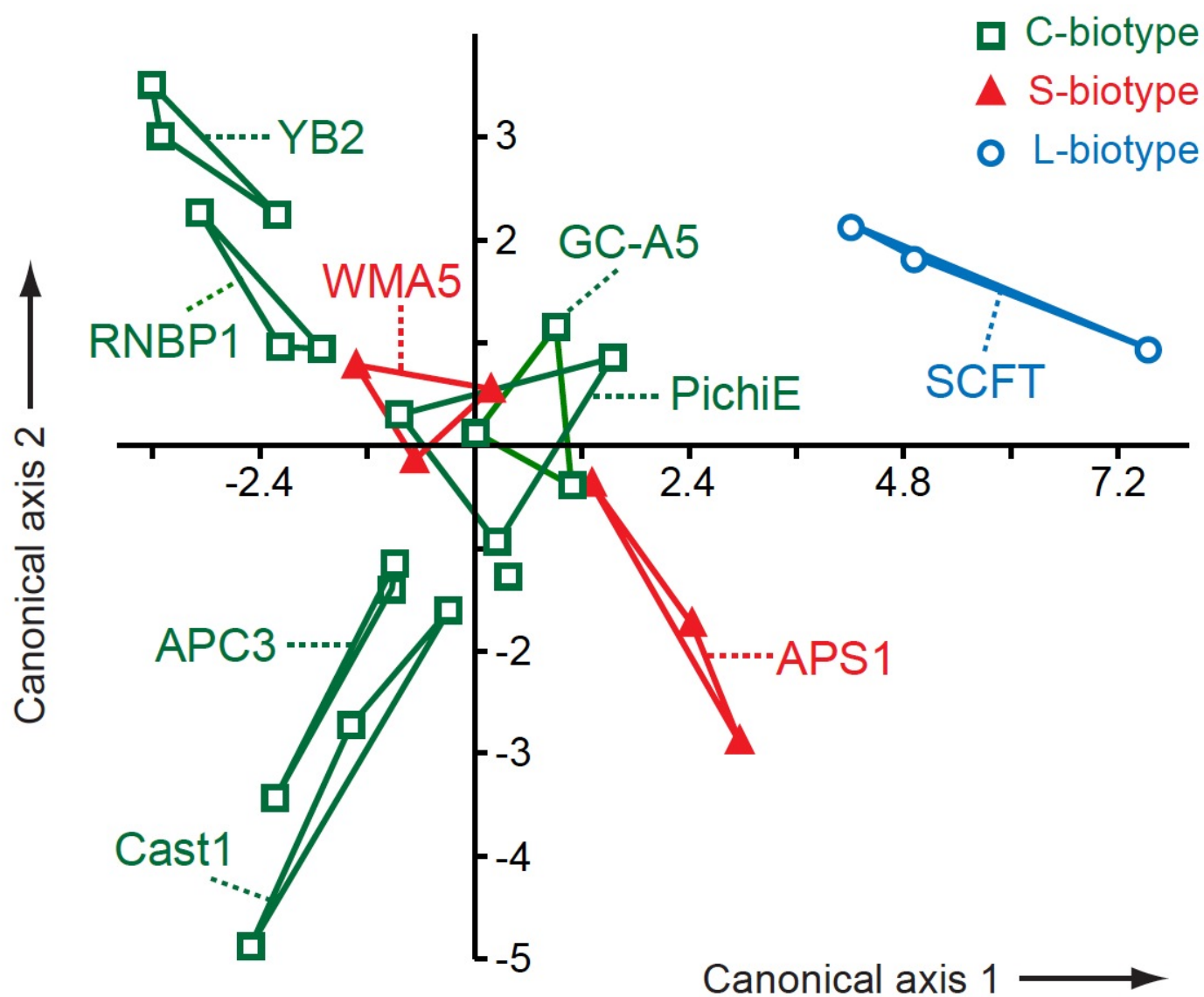


Fig 3 - Canonical variates analysis of eight PCs (68.1% of data variance) from PCA of 619 gel spots (as normalized volumes) on 27 gels. The nine fungal strains were the defined groups. Convex hulls joining data points from biological triplicate gels are labelled by strain.

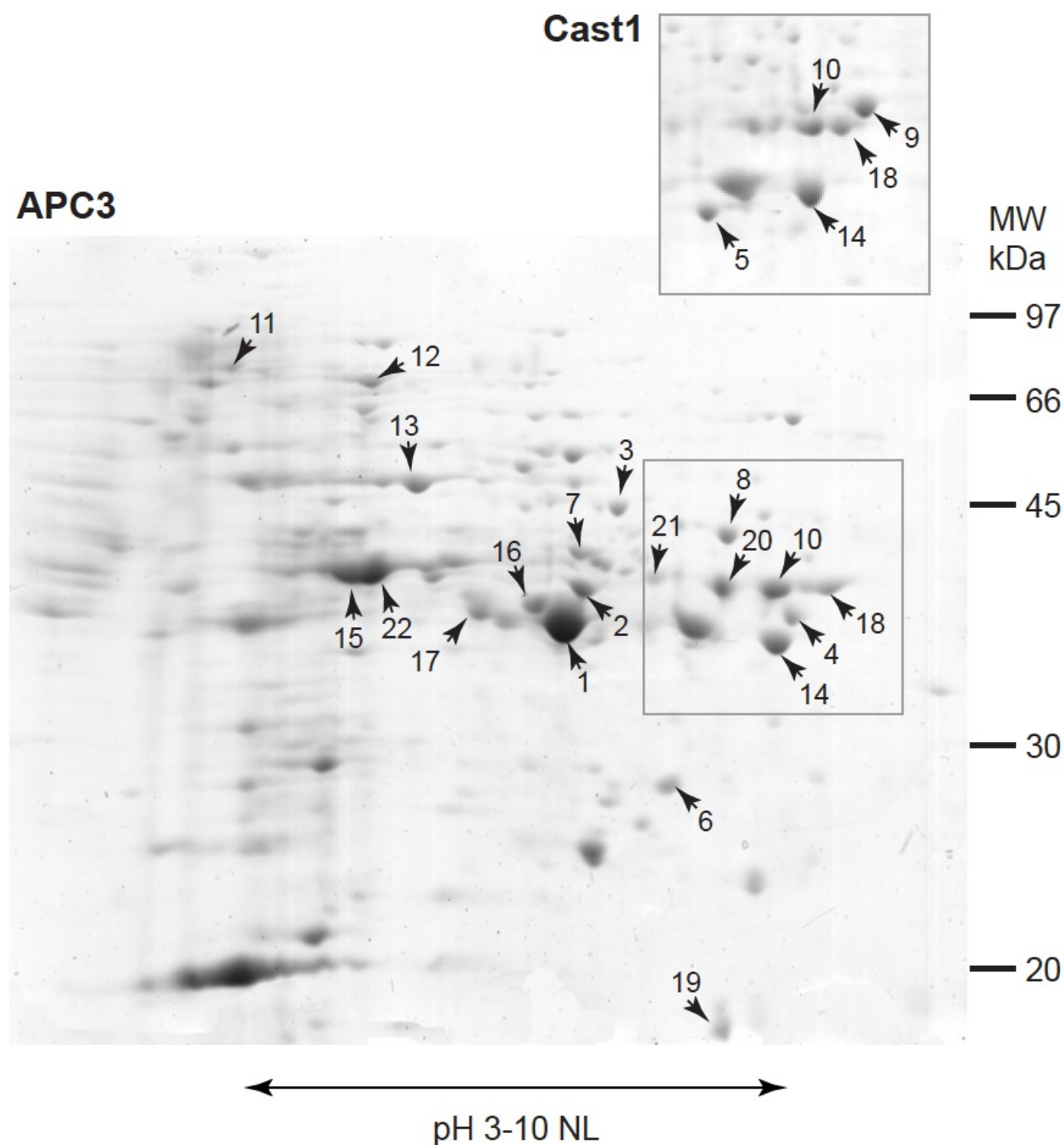


Fig 4 - 2-DE gel of proteins from cultured *M. pernicioso* strain APC3. Samples (100 ng) were subjected to isoelectric focusing in a non-linear IPG strip (7 cm, pH 3-10), then 12.5% SDS-polyacrylamide gel electrophoresis as second dimension. Proteins were stained with Coomassie Phastgel Blue R-250. Arrows indicate peptide-sequenced spots, numbered as in Tables 2-3. Inset shows part of a gel of strain Cast1 corresponding to the rectangle in the APC3 main image.